Zebrafish Ddx19 deficiency causes serious apoptosis and cell proliferation

Can Shi
Shanghai Ocean University
Linzhu Bao
Shanghai Ocean University
Yao Zu
Shanghai Ocean University
Jianfeng Ren
Shanghai Ocean University
Weiming Li
Michigan State University
Qinghua Zhang (qhzhang@shou.edu.cn)
Shanghai Ocean University https://orcid.org/0000-0002-6416-9134

Research article

Keywords: Zebrafish, CRISPR/Cas9, DEAD-box RNA helicases, Apoptosis, Cell proliferation

Posted Date: July 2nd, 2019

DOI: https://doi.org/10.21203/rs.2.10830/v1

Abstract

Background: DDX19 is known as for its role in mRNA transport. It is also involved in translation and innate immune responses. However, the function of Ddx19 during body development rarely reported. We know that ddx19 plays an important role in development of organisms, but we don't understand how it affects the process of cell development. Results: Here, we report ddx19-deleted mutation in zebrafish, obtained two types with base deletion of 46 bp and 7 bp using CRISPR/Cas9 gene knockout technology, show morphologic defects such as small head, small eyes, pericardial edema and trunk curvature in 24 hours post fertilization (hpf). The maximum survival time of ddx19 -/- was less than 5 day post fertilization (dpf). In comparison to the wildtype, the mutant embryos showed widespread up-regulation of cell apoptosis, and significant decrease in the number of cells. Conclusions: These data indicate loss of ddx19 is lethal, and is associated with cell apoptosis and proliferation abnormalities in the organism. Our results reveal that ddx19 is essential for the development of zebrafish embryos, which deepens the understanding of the developmental function of DEAD-box genes family.

Background

The DEAD-box is a large protein family characterized by its Asp-Glu-Ala-Asp (DEAD) motif. This RNA helicase family is highly conserved from prokaryotic microorganisms to eukaryotes [1], with broad functions in RNA metabolism [2]. Numerous reports have shown that some members in this family play multiple roles in the nuclear-cytoplasmic transport process [3, 4], tumorigenesis[5-7] and cell growth[8-10]. However, the function and mechanism of most members in organism development remain largely unknown or examined through *in vivo* studies.

DDX19 also known as Dbp5 in yeast, is a DEAD-box protein that plays an important role in the mRNA transport [11-13]. DDX19 is mainly found in the cytoplasm and enriched at the nuclear envelope as a component of NPC in yeast [14, 15]. Human DDX19 contains an N-terminal extension (NTE) and two RecA domains, it undergoes conformational transformation and forms the RNA-bound conformation under the binding effects of Gle1, Nup42 and Nup214 [16, 17]. Blocking of mRNA transport will seriously affects cellular functions. Knockdown of DBP5/DDX19 by siRNA in U2OS cells results in an increase in the number of cells in G1-phase, and changes in mRNAs transcripts in the cytoplasm [18]. In 2013, Jao, L.E. et al.. obtained the *ddx19* $^{-/-}$ using CRISPR/Cas9 gene editing technology that mediated multiple allele knockouts in zebrafish genome, and found that *ddx19* gene knockout leads to phenotypic defects and homozygous death [19]. However, which cell processes are involved in *ddx19* and how *ddx19* affects cell development *in vivo* remain to be explored.

Previous studies have linked DEAD-box proteins to cell apoptosis and cell proliferation [8, 10, 20-22], two cellular processes that manifest growth and development. Apoptosis, or programmed cell death, is a physiological processes closely related to cancer, autoimmunity and degenerative diseases. This process is initiated and regulated by the caspase family, which is composed of seven proteins in zebrafish [23] and activated through a variety of independent pathways. The internal mitochondrial pathway, death receptor-mediated external pathway, and endoplasmic reticulum pathway are all known to mediate apoptosis [24-26]. Cell proliferation is often regulated by the cell cycle. As a conserved mechanism of eukaryotic cell self-replication, cell cycle regulation is crucial for tissue homeostasis and cell replacement during organism development. Multiple regulatory factors are involved in the cell cycle regulation process [27]. Any wrong expression of these factors likely will lead to malignant proliferation and differentiation, which are associated with a variety of diseases and tumors. Such as, cell proliferation and tumorigenesis of esophageal cancer are inhibited in *ddx5* $^{-/-}$[7]; Overexpression DDX20 promotes the proliferation of prostate cancer cells through the NF-κB pathway [8].

Here, we hypothesized that the mRNA transport factor Ddx19 regulates the process of cell proliferation and apoptosis, and consequently affects body development in zebrafish. We tested this hypothesis by deleting *ddx19* in zebrafish, using CRISPR/Cas9 gene editing technology. We obtained two types of deletion mutated phenotypes with apparent development defects. Both types survived up to 4-5 dpf and showed up-regulation in apoptosis levels and decreased numbers of cells in the S-phase.

Results

Ddx19was persistently expressed in zebrafish embryos

The amino acid residues of Ddx19 were 89% identical in human, mouse and zebrafish (Fig.1a). Only one *ddx19* gene was found in zebrafish, although two homologous genes *(DDX19A/Ddx19a)* and (*DDX19B/Ddx19b)* have been identified in human and mouse (Fig.1b). To confirm the expression of *ddx19* in early development of zebrafish, we measured *ddx19* mRNA transcripts in the embryos by q-RT PCR firstly. The *ddx19* mRNA was present from the 1-cell stage to 125 hpf (Fig.1c-d). The expression level of *ddx19* decreased from the 1-cell stage to the 6-somite stage (Fig.1c). In comparison to 24 hpf, the expression level was higher during 24-125 hpf, and subsequently became less variable (Fig. 1d). We speculated that *ddx19* may play a role in early embryonic development of zebrafish.

The *ddx19* gene was knocked out using CRISPR/Cas9

The total length of *ddx19* gene was 13424bp, with 12 exons, of which the first exon was targeted using CRISPR/Cas9 (Fig.2a). The non-injected WT group showed one band using T7E1 enzyme digestion, and the sequencing peak was single, while T7E1 enzyme digestion showed three bands, which were 472bp, 196bp and 176bp, respectively (Fig.2b) and the sequencing peak was chaotic near the target in positive F_0 (Fig.2c).

The F_0 positive was mated with the wildtype to produce F_1 offspring. Electrophoresis analyses of fin clips DNA showed two bands in heterozygotes (Fig.3a). Sequence analyses of the cDNA showed two types of mutants, with 7 bp and 46 bp deletion, respectively (Fig.3b). Furthermore, we analyzed the protein structure of Ddx19 in wildtype and mutants. Ddx19 had 487 amino acids, contained DEXDc and HELICc two domain, with five conserved motifs. Both types of deletion caused frame-shift mutation and premature termination (Fig.3c). The *ddx19* in the mutation of 7 bp deletion coded 17 amino acids while the *ddx19* in the 46 bp deletion mutants was missing the starting codon.

Ddx19 was essential for embryonic development of zebrafish

Compared with the control group, the 10-tailed zebrafish in the experimental group showed morphologic defect (Fig.4a). We further verified the corresponding relationship between genotype and phenotype, and found that all morphological defects were corresponding to *ddx19* $^{-/-}$ (Fig.4b). Compared with the control groups, the *ddx19* $^{-/-}$ mutants showed smaller heads, smaller eyes, pericardial edema and trunk curvature. When the mutants were injected with 100-250 ng/μL *ddx19* mRNA in the 1-cell stage, the morphologic defects observed in the negative control was rescued completely (Fig.5a), Compared to the control group, the experimental group rescued with *ddx19* mRNA injection showed a decreased proportion of phenotypic defects (p = 0.029, ^{2}-test; Fig. 5b). We quantified *ddx19* transcripts by q-PCR in the wild type and *ddx19* $^{-/-}$, and detected that its transcription level was significantly decreased in *ddx19* $^{-/-}$ (p = 0.007, Student t-test; Fig.5c).

We counted defect phenotypes in the offspring from three pairs of parents and calculated the proportion in the total. The proportion of phenotypic defects was about 20%. Our data supports that the phenotypes consistent with Mendelian's law in the *ddx19* $^{-/-}$ with 46 bp deletion (p = 0.970, ^{2}-test; Fig.6a). The same conclusion was reached in the *ddx19* $^{-/-}$ with 7bp deletion (p = 0.970, ^{2}-test; Fig.6b). We counted the number of daily deaths of zebrafish with phenotypic defects and analyzed their vitality. The result showed that the maximum survival time of *ddx19* $^{-/-}$ missing 46 bp was no more than 4 dpf (Fig.6c), and the maximum survival time of *ddx19* $^{-/-}$ missing 7 bp was no more than 5 dpf (Fig.6d).

Apoptotic signals were up-regulated and cell proliferation was decreased in *ddx19* $^{-/-}$

Compared with the wildtype (Fig.7a), apoptotic signals were up-regulated in *ddx19* $^{-/-}$ missing 46 bp at 24 hpf (Fig.7b), and *ddx19* $^{-/-}$ missing 7 bp showed the same performance (Fig.7c). Apoptosis was widespread throughout the body in *ddx19* $^{-/-}$ at 24 hpf (Fig.S1a), while the apoptosis signal decreased in *ddx19* $^{-/-}$ at 48 hpf than that at 24 hpf (Fig.S1b). At 48hpf, confocal imaging showed that unlike cell proliferation in wildtype groups (Fig.8a), partial embryos of *ddx19* $^{-/-}$ sibling were detected a decrease in the number of cells in S-phase, suggesting that cell proliferation may be blocked in *ddx19* $^{+/-}$ (Fig.8b), and the number of cells in S-phase was significantly decrease in *ddx19* $^{-/-}$, indicating that cell proliferation was significantly blocked (Fig.8c). Our results were confirmed by repeated experiments (Fig.S2a-b). The detection results of 60hpf were also consistent with 48hpf (Fig.S2c).

Discussion

Here we have shown that the deletion of *ddx19* causes abnormal apoptosis and proliferation in zebrafish embryos, and subsequently death. The phenotypes from our *ddx19* $^{-/-}$ are similar to that of homozygous *ddx19* mutants (*ddx19*$^{hi1464/hi1464}$), resulting in phenotypic defects and homozygous death [28]. In addition to these findings, we found that the absence of DDX19 caused in the arrest of cells in the S-phase. The *ddx19* $^{-/-}$ appeared to have more serious defects in body development, and this could be a reason of early death in embryos. It is also possible that abnormality of apoptosis and cell proliferation contributed to deformity of embryonic development and death in *ddx19* $^{-/-}$.

The mechanism for causing changes in apoptosis and cell proliferation is not known. Here, we suggest a possible mechanism which DNA damage results in apoptosis and abnormal cell proliferation. Some studies have shown that R-loop may be a major source of replication stress and genomic instability, leading to DNA damage responses [29-31]. The regulation of R-loop levels is complex and varied. Depletion of RNase H activity impairs the removal of R-loop in saccharides, causing DNA damage [32]. Helicase DHX9 interacts with PARP1 to prevent R-loop dependent DNA damage. The integrity of DNA is the key to the survival and reproduction of organisms [33]. Therefore, the repair of DNA damage is very important. Many researchers have found that DNA damage response is often accompanied by apoptosis and abnormal cell proliferation [34-38]. The DNA damage checkpoint kinases Chk1 and Chk2 are closely related to apoptosis and cell cycle [39]. Overexpression of E2F3a induces DNA damage, leading to ATM-dependent apoptosis [40]. Here, we focused on the functionality of Ddx19. According to the report that Ddx19 cleared the R-loop caused by DNA damage to stabilized genomic DNA in HeLa cells [31]. Ddx19 acts as a bridge between mRNA nuclear export and transcription and replication, inhibiting genomic instability after DNA damage in proliferating cells [41]. Combined with our findings on its role in the process of apoptosis and proliferation, we speculate that *ddx19* deletion induces DNA damage due to the R-loop accumulation. This leads to widespread cell apoptosis and proliferation abnormalities, leading to death of zebrafish embryos and larvae. To test this hypothesis, the next work can be perform

by construct a fusion protein of the DNA-RNA hybrid binding domain to further examine whether R-loop accumulated in *ddx19* $^{-/-}$, and to detect and compare the expression of DNA damage checkpoint protein kinases in wildtype and *ddx19* $^{-/-}$.

Many members of the DEAD-box family are known to regulate development [42-46]. For example, Ddx27 deletion blocked proliferation and regeneration ability of skeletal muscle in zebrafish [42]. Loss of Ddx18 results in G1 cell-cycle arrest, and specifically regulates the amount of primitive myeloid and erythroid cells [45]. Unlike Ddx19, Ddx27 and Ddx18 are mainly involved in the ribosomal biogenesis process. Ddx46 is related to the splicing of pre-mRNA, and is required for development of digestive organs and brain as well as differentiation of hematopoietic stem cells in zebrafish [43, 44]. Ddx39ab, also known as a nucleoplasm transport factor, specifically participates in myocyte and lens development in zebrafish, and its deletion blocked mRNA splicing of members of the kmt2 gene family [46]. Similar to *ddx19* $^{-/-}$, the homozygous death of *ddx39ab* occurs at an early developmental stage. But the defect phenotypes caused by *ddx19* $^{-/-}$ are more extensive and severe than those caused by of *ddx39ab* $^{-/-}$. Nucleoplasm transport factor DDX3 maintains cell cycle and genome stability in HCT116 [28], and our observation of the roles of Ddx19 during development *in vivo* was similar to it. Therefore, we speculated that the nucleoplasm transport factor in the DEAD-box family may be involved in the regulation of apoptosis and proliferation, which provided a theoretical reference for our further understanding and classify of the family.

Conclusion

We obtained *ddx19* heritable effective mutants by CRISPR/Cas9 genome editing technology in zebrafish. The *ddx19* $^{-/-}$ were lethal. *ddx19* knockout caused severe deformity, up-regulation in apoptosis, a significant decrease in the number of cells in the S-phase, and largely blocking of cell proliferation. We conclude that Ddx19 is involved in the regulation of cell apoptosis and proliferation, thus affecting the normal development process in zebrafish embryos and larvae.

Methods

Zebrafish source and maintenance

The experimental wildtype zebrafish was the AB strain, purchased from Shanghai Institute of Biochemistry and Cell Biology. Zebrafish was handled according to the procedures of the Institutional Animal Care and Use Committee of Shanghai Ocean University, Shanghai, China and maintained according to standard protocols (http://zfin.org).

Gene knockout by CRISPR/Cas9 method

The gRNA plasmid used for gene knockout was a gift from Prof. Jingwei Xiong of Peking University. The pUC19-scaffold plasmid sequence is GTTTTAGAGCTAGAAATAGCAAGTTAAAATAAGGCTAGTCCGTTATCAACTTGAAAAAGTGGCACCGAGTCGGTGCTTTTTTT.

The MAXIscriptt ® T7 *in vitro* Transcription Kit (Ambion, AM1314) was used for RNA synthesis in this study. The upstream primer sequences of gRNA was

5′-TAATACGACTCACTATAGGCAACAGATTCGTGGGCCCGTTTTAGAGCTAGAAATAGC-3′. The downstream primer was universal primer, which sequences was 5′-AAAAAAAGCACCGACTCGGTGCCAC-3′. We designed the targeting sequence consistent with previous studies [19]. gRNA was synthesized by *in vitro* transcription, and co-injected with Cas9 protein

into the animal pole at the one-cell stage. The final concentration of gRNA for injection was 100 ng/μL and Cas9 protein was 800 ng/μL, and the injection volume was 1nL.

Genotyping

DNA was extracted from fin clips or single embryos by NaOH solution cleavage, used for genotyping using PCR. The primers sequences for genotyping were 5'-GTGTGAGACTCGCAACCCAT-3' and 5'- ACCACAATATTAGTACAGCAACACT-3'.

mRNA rescue experiment

The mRNA used in the experiment was full-length sequences of the whole coding region. The primer sequence for mRNA synthesize was 5'- CGGGGTACCTTTAAAAAGAAGGACATGGCAAC-3' and 5'-CGGACTAGTGT-

AAACGTCACAGGCGGAC-3'. The PCR product was inserted to the pXT7 plasmid. The recombinant plasmids were sequenced, linearized and purified. mRNA was synthesized by *in vitro* transcription using the mMESSAGE mMACHINE T7 ULTRA kit (Ambion, AM1344). Similar to those for gene knockout, 100-250 ng/μL *ddx19* mRNA was injected into animal polar at the one-cell stage of zebrafish. Embryos obtained by hybridization of *ddx19* heterozygous mutants. The phenotypes were observed and photographed, and the corresponding genotypes were identified one by one at 48hpf. To analyzed whether the phenotypic defects of *ddx19* $^{-/-}$ has been rescued

Quantitative RT-PCR

RNA was extracted from each group of 10-20 embryos by TRIZOL reagent (Invitrogen□15596-018). cDNA was obtained by the Prime Script ^{TM} RT reagent Kit with gDNA Eraser (TAKARA, RR047A). Light Cycler $^{®}$ 480 II of Roche was used to conduct fluorescence quantitative experiments with the SYBR Green Master Mix (Roche, 6924204001), and *β-actin* was the reference gene. Three biological replicates were performed in each group. All experimental operations were carried out in accordance with the venders' instructions.

TUNEL staining

Cell apoptosis was assayed using the *In Situ* Cell Death Detection Kit (Roche, 11684795910). Embryos were collected at 24 hpf and 48 hpf and fixed with 4% PFA-PBS overnight at 4 °C, and subsequently washed with PBST, and incubated with protease k for 15-30 min. After the reaction was terminated, the samples were fixed again at room temperature for 20 min and TUNEL stained over night at 37 °C. We washed away the TUNEL reaction solution using 1x hoechst $^{®}$ 33342 solution incubation 2 h at 37 °C. Finally, samples were fixed with 1%-1.5% low melting glue and photographed under a confocal microscope.

Edu labeling

Edu labeling was carried out as described [42]. We analyzed the proliferating cells in zebrafish embryos using Click-iT $^{®}$ Plus Edu Imaging Kits (Invitrogen, C10639). Embryos of 24 dpf were incubated for 3 h at a concentration of 400 μm Edu. We removed the Edu label solution, collected embryos at 48 hpf and 60 hpf, fixed with 4% PFA-PBS overnight at 4 °C. Then, the samples were incubated with protease k for 15-30 min at room temperature. The samples were fixed again

for 20 min at room temperature. The detection reaction solution is proportionally configured according to the requirements of the instruction, and fully mixed. Samples were incubated overnight at 37 °C. We removed the reaction solution, and incubated the samples in 1x hoechst ® 33342 solution (final concentration 5 g/mL) for 2 h at 37 °C. Samples were fixed with 1%-1.5% low melting glue. Samples were examined with confocal photography.

Imaging

Images were obtained using Zeiss Axio Imager2. A Leica TCS SP8 laser scanning confocal microscope was used for fluorescence imaging.

Statistical analysis

All experimental results were from three or more biological replicates. Phenotypic analysis was performed using the ^{2}-test. Student t-test was used for the pairwise difference analysis. Results were considered significant when $p<0.05$.

Declaration

Acknowledgements

We are grateful to professor Jingwei Xiong of Peking University for providing the pUC19-scaffold plasmid. We thank Jing Xie for maintenance of the laboratory and the fish care and members of our laboratory for comment and modify on the writing.

Funding

Research was supported by the ministry of education returnees research fund (D-8002-15-0042), China-US Ocean Research Center Fund (A1-0209-15-0806), Shanghai first-class discipline construction fund and the National Natural Science Foundation of China (No. 31501166).

Availability of data or materials

All datasets on which the conclusions of the manuscript rely are presented in the main paper and supplementary figures.

Authors’ contributions

The whole experiments was designed and performed by Can Shi. Weiming Li, Qinghua Zhang participated in study design and finalized the Manuscript. Yao Zu and Jianfeng Ren directed the experiments. Linzhu Bao assisted with the experiments. Both authors read and approved the final manuscript.

Ethics approval and consent to participat

Zebrafish was handled according to the procedures of the Institutional Animal Care and Use Committee of Shanghai Ocean University, Shanghai, China and maintained according to standard protocols (http://zfin.org). Use of Zebrafish and the research methods were approved by the Shanghai Ocean University Experimentation Ethics Review Committee (SHOU-DW-2016-002).

Consent for publication

Not applicable.

Competing interests

The authors declare that they have no competing interests.

Publisher's Note

References

1. Jankowsky E, Fairman ME: RNA helicases–one fold for many functions. *Curr Opin Struct Biol* 2007, 17(3):316-324.

2. Linder P: Dead-box proteins: a family affair–active and passive players in RNP-remodeling. *Nucleic Acids Res* 2006, 34(15):4168-4180.

3. Frohlich A, Rojas-Araya B, Pereira-Montecinos C, Dellarossa A, Toro-Ascuy D, Prades-Perez Y, Garcia-de-Gracia F, Garces-Alday A, Rubilar PS, Valiente-Echeverria F *et al*: DEAD-box RNA helicase DDX3 connects CRM1-dependent nuclear export and translation of the HIV-1 unspliced mRNA through its N-terminal domain. *Biochim Biophys Acta* 2016, 1859(5):719-730.

4. Zonta E, Bittencourt D, Samaan S, Germann S, Dutertre M, Auboeuf D: The RNA helicase DDX5/p68 is a key factor promoting c-fos expression at different levels from transcription to mRNA export. *Nucleic Acids Res* 2013, 41(1):554-564.

5. Jiang F, Zhang D, Li G, Wang X: Knockdown of DDX46 Inhibits the Invasion and Tumorigenesis in Osteosarcoma Cells. *Oncol Res* 2017, 25(3):417-425.

6. Li B, Li YM, He WT, Chen H, Zhu HW, Liu T, Zhang JH, Song TN, Zhou YL: Knockdown of DDX46 inhibits proliferation and induces apoptosis in esophageal squamous cell carcinoma cells. *Oncol Rep* 2016, 36(1):223-230.

7. Ma Z, Feng J, Guo Y, Kong R, Ma Y, Sun L, Yang X, Zhou B, Li S, Zhang W *et al*: Knockdown of DDX5 Inhibits the Proliferation and Tumorigenesis in Esophageal Cancer. *Oncol Res* 2017, 25(6):887-895.

8. Chen W, Zhou P, Li X: High expression of DDX20 enhances the proliferation and metastatic potential of prostate cancer cells through the NF-kappaB pathway. *Int J Mol Med* 2016, 37(6):1551-1557.

9. Wang X, Liu H, Zhao C, Li W, Xu H, Chen Y: The DEAD-box RNA helicase 51 controls non-small cell lung cancer proliferation by regulating cell cycle progression via multiple pathways. *Sci Rep* 2016, 6(26108):1-10.

10. Zhen Z, Zhang M, Yuan X, Qu B, Yu Y, Gao X, Qiu Y: DEAD-box helicase 6 (DDX6) is a new negative regulator for milk synthesis and proliferation of bovine mammary epithelial cells. *In Vitro Cell Dev Biol Anim* 2018, 54(1):52-60.

11. Mehta J, Tuteja R: A novel dual Dbp5/DDX19 homologue from Plasmodium falciparum requires Q motif for activity. *Mol Biochem Parasitol* 2011, 176(1):58-63.

12. Montpetit B, Thomsen ND, Helmke KJ, Seeliger MA, Berger JM, Weis K: A conserved mechanism of DEAD-box ATPase activation by nucleoporins and InsP6 in mRNA export. *Nature* 2011, 472(7342):238-242.

13. Tran EJ, Zhou Y, Corbett AH, Wente SR: The DEAD-box protein Dbp5 controls mRNA export by triggering specific RNA:protein remodeling events. *Mol Cell* 2007, 28(5):850-859.

14. Hodge CA, Colot HV, Stafford P, Cole1 CN: Rat8p/Dbp5p is a shuttling transport factor that interacts with Rat7p/Nup159p and Gle1p and suppresses the mRNA export defect of xpo1-1 cells. *The EMBO Journal* 1999, 18(20):5778–5788.

15. Schmitt C, Kobbe CV, Bachi A, Pante´ N, Rodrigues JP, Boscheron CC, Rigaut G, Wilm M, Se´raphin B, Carmo-Fonseca M *et al*: Dbp5, a DEAD-box protein required for mRNA export, is recruited to the cytoplasmic fibrils of nuclear pore complex via a conserved interaction with CAN/Nup159. *The EMBO Journal* 1999, 18(15):4332–4347.

16. Lin DH, Correia AR, Cai SW, Huber FM, Jette CA, Hoelz A: Structural and functional analysis of mRNA export regulation by the nuclear pore complex. *Nat Commun* 2018, 9(2319):1-19.

17. Napetschnig J, Kassube SA, Debler EW, Wong RW, Blobel G, Hoelz A: Structural and functional analysis of the interaction between the nucleoporin Nup214 and the DEAD-box helicase Ddx19. *PNAS* 2009, 106(9):3089–3094.

18. Okamura M, Yamanaka Y, Shigemoto M, Kitadani Y, Kobayashi Y, Kambe T, Nagao M, Kobayashi I, Okumura K, Masuda S: Depletion of mRNA export regulator DBP5/DDX19, GLE1 or IPPK that is a key enzyme for the production of IP6, resulting in differentially altered cytoplasmic mRNA expression and specific cell defect. *PLoS One* 2018, 13(5):1-24.

19. Jao LE, Wente SR, Chen W: Efficient multiplex biallelic zebrafish genome editing using a CRISPR nuclease system. *Proc Natl Acad Sci U S A* 2013, 110(34):13904-13909.

20. Kim H, Kim Y, Jeoung D: DDX53 Promotes Cancer Stem Cell-Like Properties and Autophagy. *Mol Cells* 2017, 40(1):54-65.

21. Redmond AM, Byrne C, Bane FT, Brown GD, Tibbitts P, O'Brien K, Hill AD, Carroll JS, Young LS: Genomic interaction between ER and HMGB2 identifies DDX18 as a novel driver of endocrine resistance in breast cancer cells. *Oncogene* 2015, 34(29):3871-3880.

22. You J, Wang X, Wang J, Yuan B, Zhang Y: DDX59 promotes DNA replication in lung adenocarcinoma. *Cell Death Discov* 2017, 3(16095):1-11.

23. Fan T-J, Han L-H, Cong R-S, Liang J: Caspase Family Proteases and Apoptosis. *Acta Biochimica et Biophysica Sinica* 2005, 37(11):719-727.

24. Logue SE, Cleary P, Saveljeva S, Samali A: New directions in ER stress-induced cell death. *Apoptosis* 2013, 18(5):537-546.

25. Nagata S: Apoptosis by Death Factor. *Cell* 1997, 88:355–365.

26. Strasser A, O'Connor L, Dixit VM: APOPTOSIS SIGNALING. *Annu Rev Biochem* 2000, 69:217–245.

27. Pucci B, Kasten M, Giordano A: Cell Cycle and Apoptosis1. *Neoplasia* 2000, 2(4):291-299.

28. Chen WJ, Wang WT, Tsai TY, Li HK, Lee YW: DDX3 localizes to the centrosome and prevents multipolar mitosis by epigenetically and translationally modulating p53 expression. *Sci Rep* 2017, 7(9411):1-20.

29. Bhatia V, Barroso SI, Garcia-Rubio ML, Tumini E, Herrera-Moyano E, Aguilera A: BRCA2 prevents R-loop accumulation and associates with TREX-2 mRNA export factor PCID2. *Nature* 2014, 511(7509):362-365.

30. Hamperl S, Bocek MJ, Saldivar JC, Swigut T, Cimprich KA: Transcription-Replication Conflict Orientation Modulates R-Loop Levels and Activates Distinct DNA Damage Responses. *Cell* 2017, 170(4):774-786.

31. Hodroj D, Recolin B, Serhal K, Martinez S, Tsanov N, Abou Merhi R, Maiorano D: An ATR-dependent function for the Ddx19 RNA helicase in nuclear R-loop metabolism. *EMBO J* 2017, 36(9):1182-1198.

32. Amon JD, Koshland D: RNase H enables efficient repair of R-loop induced DNA damage. *Elife* 2016, 5(e20533):1-20.

33. Cristini A, Groh M, Kristiansen MS, Gromak N: RNA/DNA Hybrid Interactome Identifies DXH9 as a Molecular Player in Transcriptional Termination and R-Loop-Associated DNA Damage. *Cell Rep* 2018, 23(6):1891-1905.

34. Ershova ES, Jestkova EM, Chestkov IV, Porokhovnik LN, Izevskaya VL, Kutsev SI, Veiko NN, Shmarina G, Dolgikh O, Kostyuk SV: Quantification of cell-free DNA in blood plasma and DNA damage degree in lymphocytes to evaluate dysregulation of apoptosis in schizophrenia patients. *J Psychiatr Res* 2017, 87:15-22.

35. Kulms D, Zeise E, Po¨ ppelmann B, Schwarz T: DNA damage, death receptor activation and reactive oxygen species contribute to ultraviolet radiation-induced apoptosis in an essential and independent way. *Oncogene* 2002(21):5844 – 5851.

36. Saxena N, Ansari KM, Kumar R, Dhawan A, Dwivedi PD, Das M: Patulin causes DNA damage leading to cell cycle arrest and apoptosis through modulation of Bax, p(53) and p(21/WAF1) proteins in skin of mice. *Toxicol Appl Pharmacol* 2009, 234(2):192-201.

37. Seo JY, Kim DY, Kim HJ, Ryu HG, Lee J, Lee KH, Kim SH, Kim KT: Heterogeneous nuclear ribonucleoprotein (hnRNP) L promotes DNA damage-induced cell apoptosis by enhancing the translation of p53. *Oncotarget* 2017, 8(31):51108-51122.

38. Shrotriya S, Deep G, Gu M, Kaur M, Jain AK, Inturi S, Agarwal R, Agarwal C: Generation of reactive oxygen species by grape seed extract causes irreparable DNA damage leading to G2/M arrest and apoptosis selectively in head and neck squamous cell carcinoma cells. *Carcinogenesis* 2012, 33(4):848-858.

39. Urist M, Tanaka T, Poyurovsky MV, Prives C: p73 induction after DNA damage is regulated by checkpoint kinases Chk1 and Chk2. *Genes Dev* 2004, 18(24):3041-3054.

40. Paulson QX, Pusapati RV, Hong S, Weaks RL, Conti CJ, Johnson DG: Transgenic expression of E2F3a causes DNA damage leading to ATM-dependent apoptosis. *Oncogene* 2008, 27(36):4954-4961.

41. Hodroj D, Serhal K, Maiorano D: Ddx19 links mRNA nuclear export with progression of transcription and replication and suppresses genomic instability upon DNA damage in proliferating cells. *Nucleus* 2017, 8(5):489-495.

42. Bennett AH, O'Donohue MF, Gundry SR, Chan AT, Widrick J, Draper I, Chakraborty A, Zhou Y, Zon LI, Gleizes PE *et al*: RNA helicase, DDX27 regulates skeletal muscle growth and regeneration by modulation of translational processes. *PLoS Genet* 2018, 14(3):1-25.

43. Hirabayashi R, Hozumi S, Higashijima S, Kikuchi Y: Ddx46 is required for multi-lineage differentiation of hematopoietic stem cells in zebrafish. *Stem Cells Dev* 2013, 22(18):2532-2542.

44. Hozumi S, Hirabayashi R, Yoshizawa A, Ogata M, Ishitani T, Tsutsumi M, Kuroiwa A, Itoh M, Kikuchi Y: DEAD-box protein Ddx46 is required for the development of the digestive organs and brain in zebrafish. *PLoS One* 2012, 7(3):1-11.

45. Payne EM, Bolli N, Rhodes J, Abdel-Wahab OI, Levine R, Hedvat CV, Stone R, Khanna-Gupta A, Sun H, Kanki JP *et al*: Ddx18 is essential for cell-cycle progression in zebrafish hematopoietic cells and is mutated in human AML. *Blood* 2011, 118(4):903-915.

46. Zhang L, Yang Y, Li B, Scott IC, Lou X: The DEAD-box RNA helicase Ddx39ab is essential for myocyte and lens development in zebrafish. *Development* 2018, 145(8):dev161018.

Figures

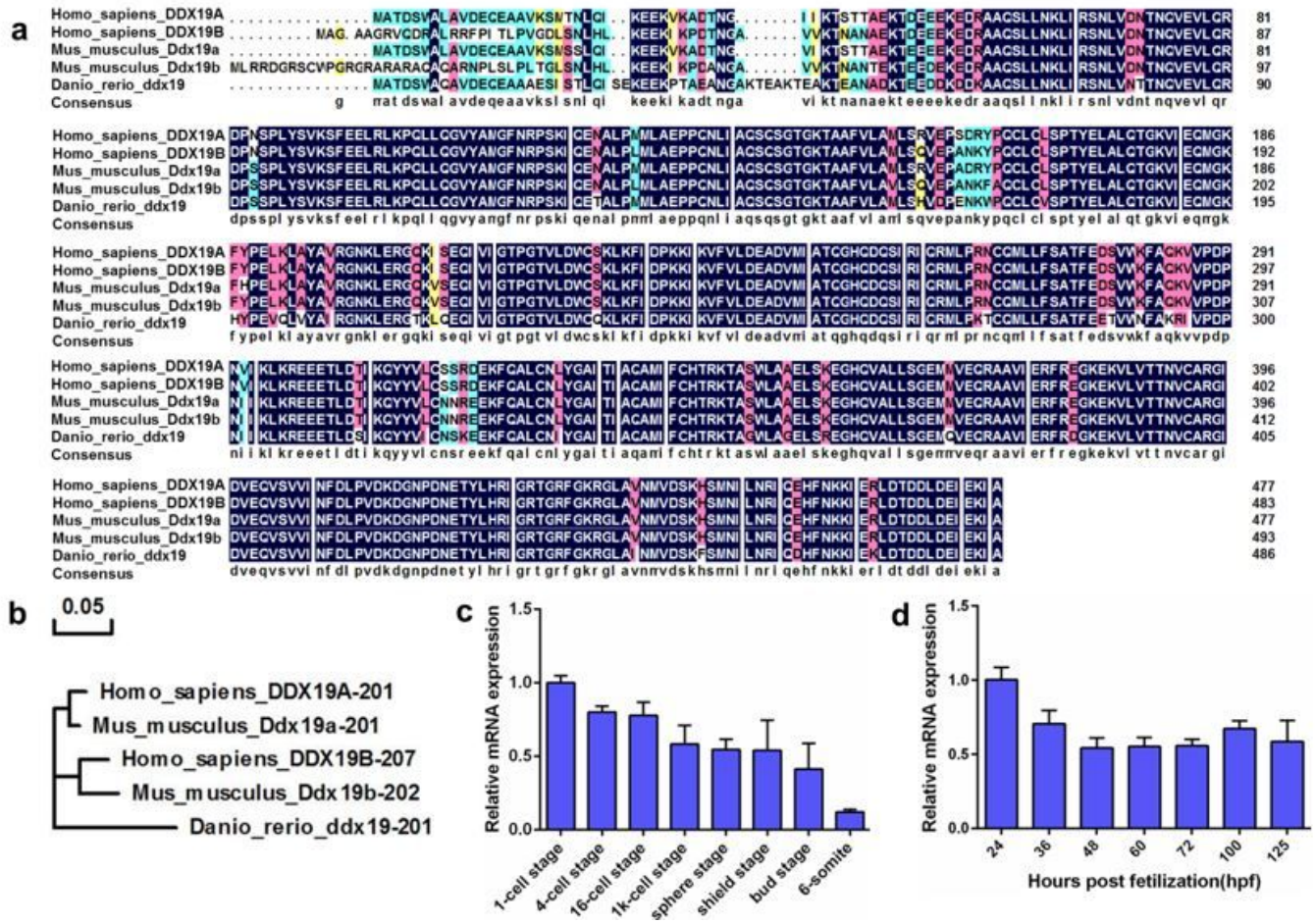

Figure 1

Ddx19 was highly conserved during vertebrate evolution and persistently expressed in early embryos of zebrafish. (a) The amino acid sequences of ddx19 in human, mouse and zebrafish were highly conserved with an identity of 89%. (b)

Evolutionary tree analysis showed that zebrafish Ddx19 was homologous to Ddx19 in human and mouse. (c) Expression of ddx19 between 1-cell and 6-somite stages. (d) Expression of ddx19 between 24-125hpf. Results of the three independent experiments were normalized to β-actin, represented by mean ± SD.

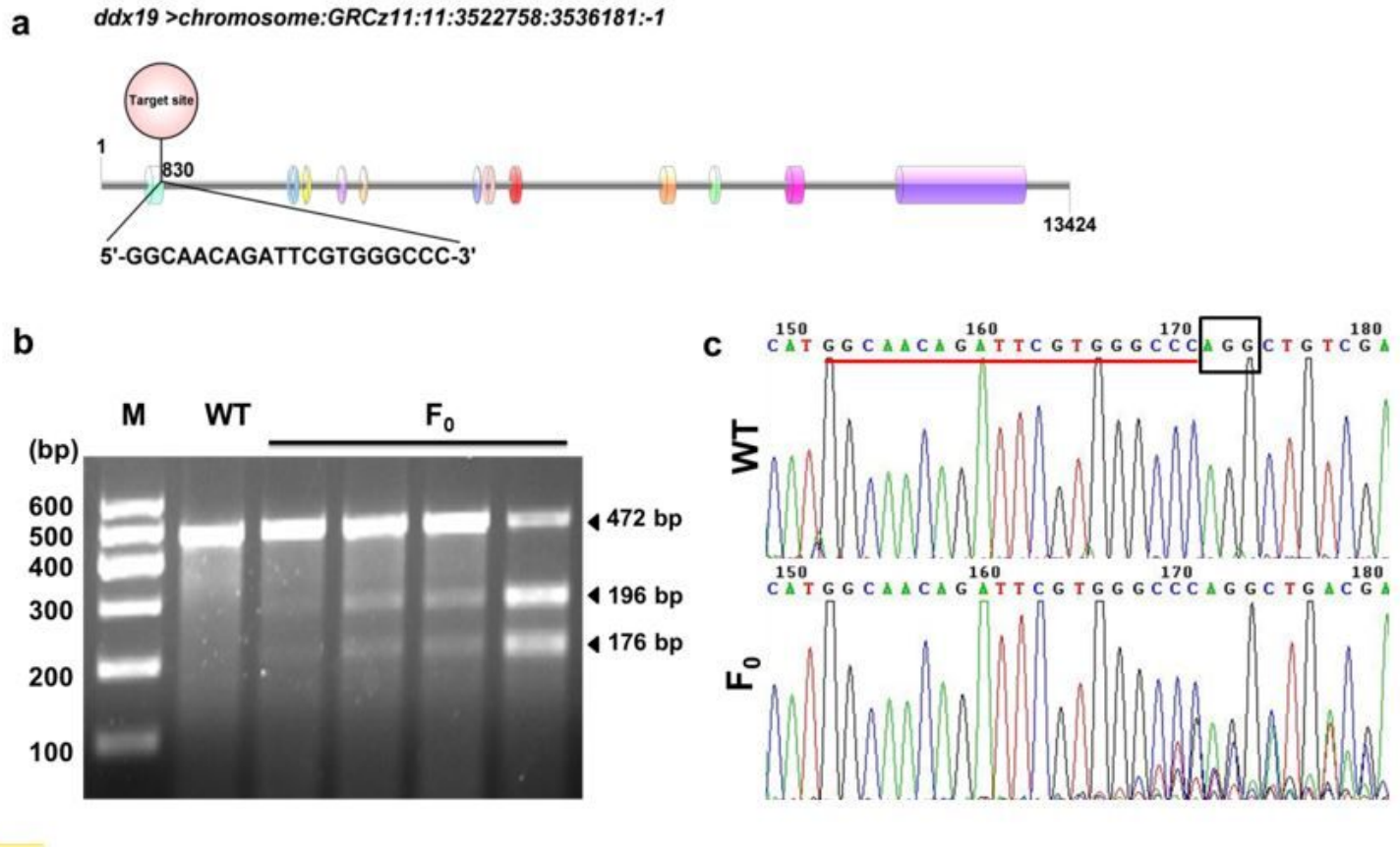

Figure 2

CRISPR/Cas9-mediated ddx19 gene knockout. (a) Target site location and sequence. There are 12 exons in the ddx19 gene, and first exon was the target locus. (b) Gel picture of electrophoresis of T7E1 detection products. The non-injected WT group showed one band, while the microinjected F0 group showed three bands after T7E1 digestion. (c) Peak map of sequencing of wildtype group and ddx19 knockout group. The red horizontal line indicates the target location, and the black box represents PAM area. Wildtype has a single peak, while peak map of F0 sequencing after microinjection showed chaotic peak after the target.

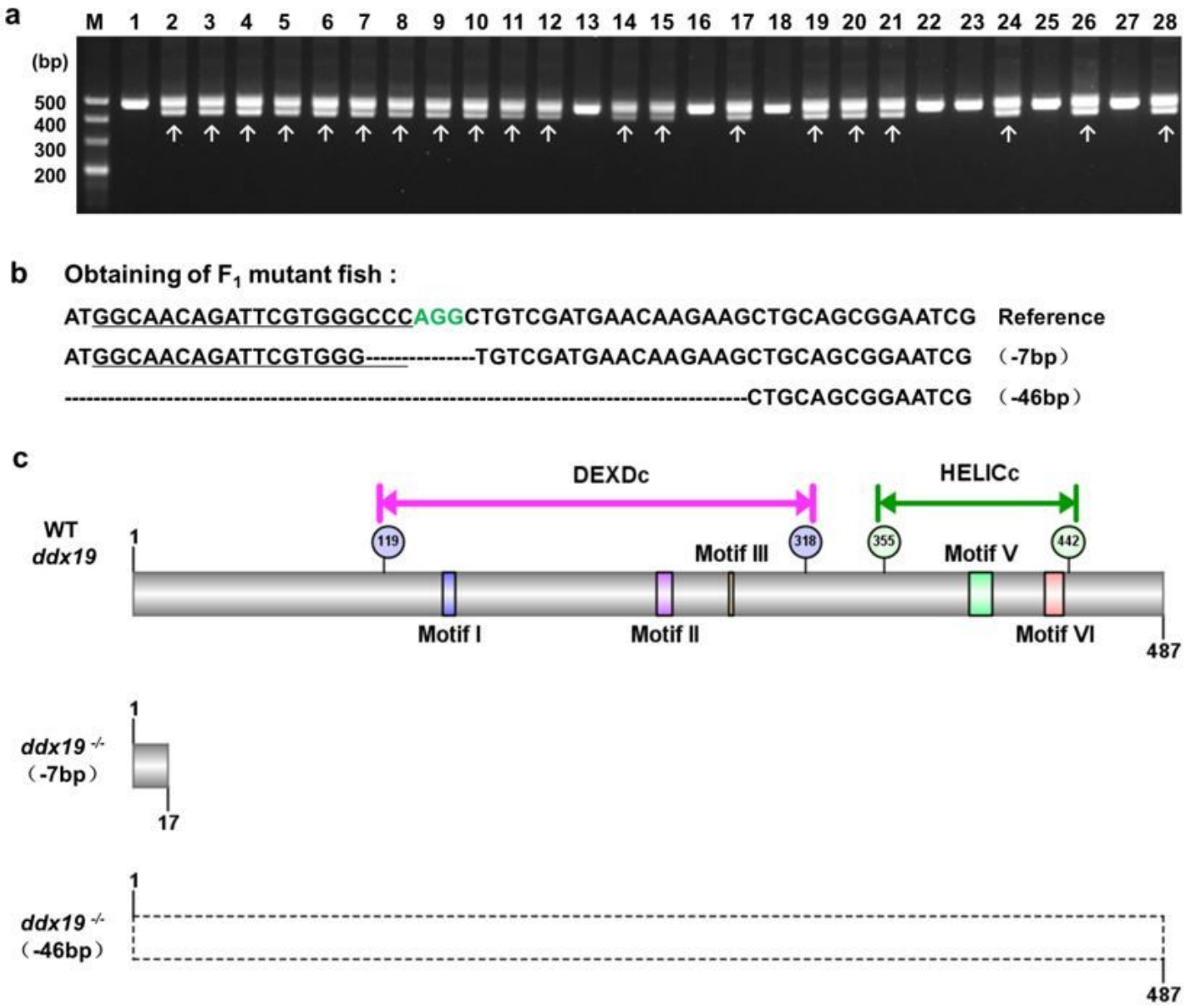

Figure 3

Screening results of ddx19 +/-. (a) Electrophoresis gel diagram of ddx19 genotype identification PCR products. ddx19 +/- with -46 bp deletion presented two electrophoretic bands. The white arrows indicate bands of heterozygous mutants. (b) Screening for different deletion types of ddx19 +/- by TA cloning and sequence alignment. Two effective mutation types were found, with 7bp and 46bp bases missing, respectively. (c) Protein structure analysis. Ddx19 contained DEXDc and HELICc domain, five conserved motifs. The deletions led to frame-shift mutations and premature termination of expression. The mutation of 7 bp deletion coded 17 amino acids while the starting codon was missing in 46 bp deletion mutants (As shown in dotted line).

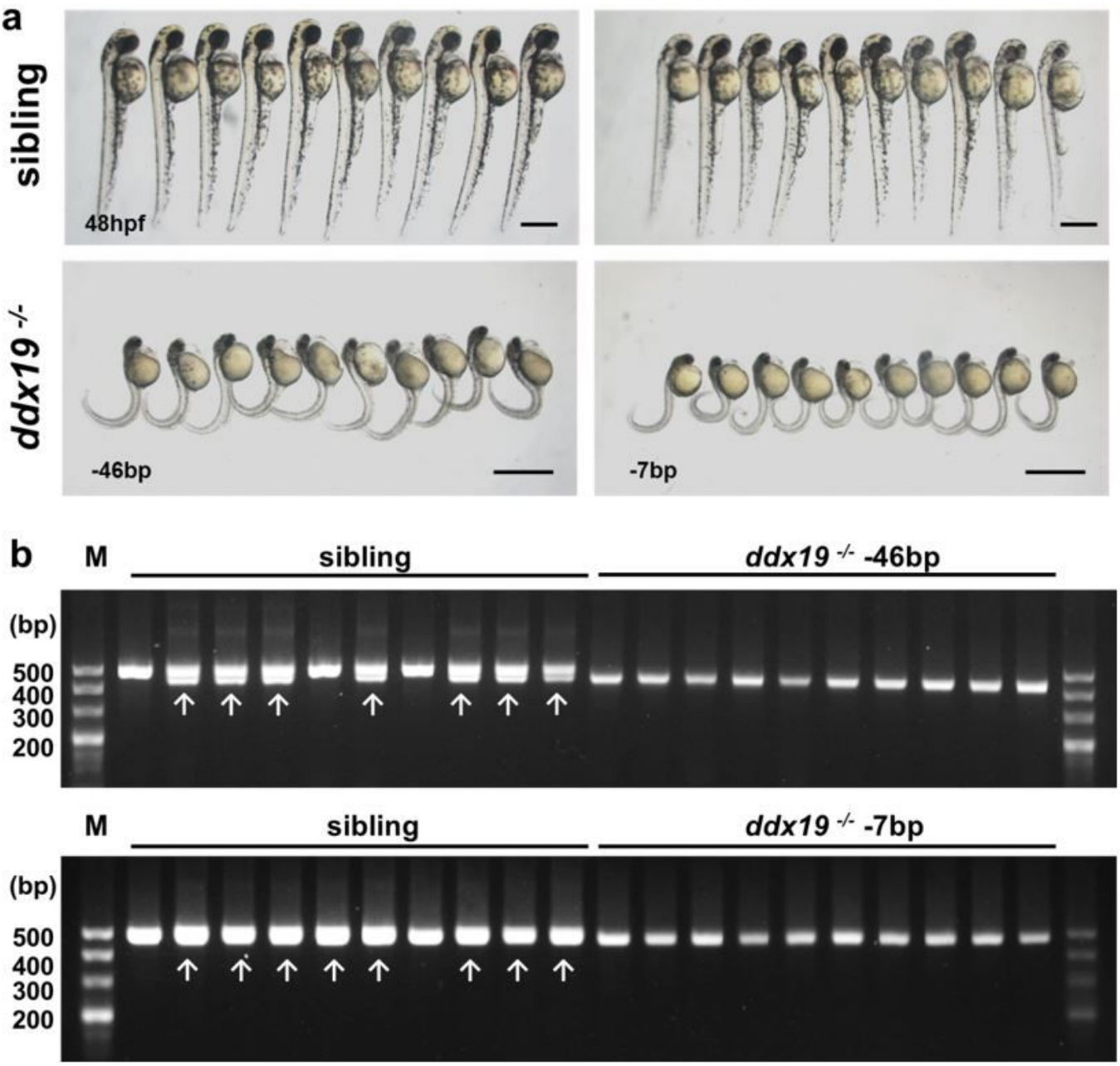

Figure 4

Genotype identification corresponding to the phenotype. (a) Group photography of different deletion types of mutants and their sibling. Scale bars are 500 μm in sibling and 1000 μm in ddx19 -/-. (b) Electrophoresis gel diagram of ddx19 genotype identification. The white arrows indicate bands of ddx19 +/-, and bands of wildtype are unlabeled in sibling group.

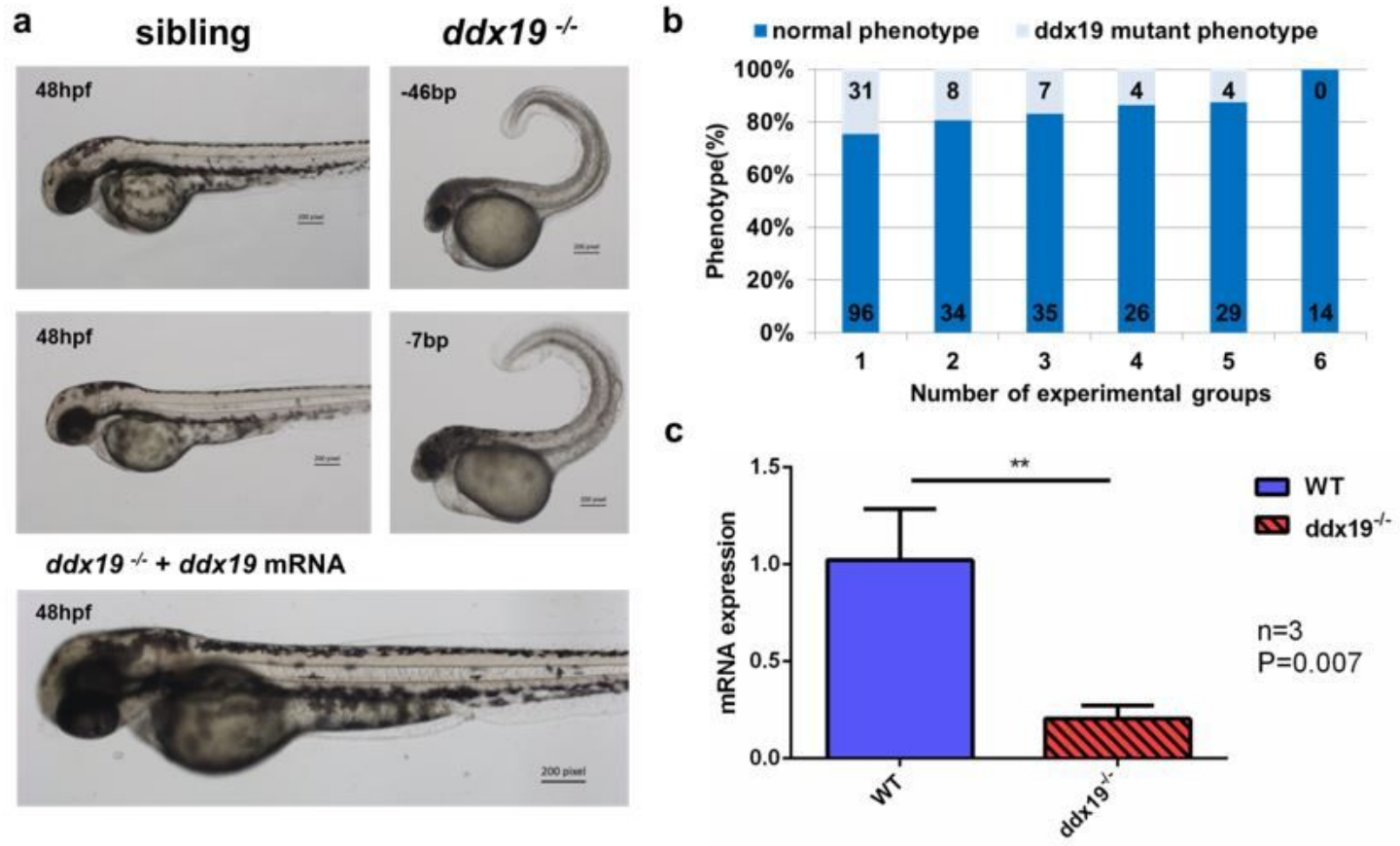

Figure 5

Loss of Ddx19 resulted in embryonic development defects in zebrafish. (a) Morphological observation of ddx19 homozygous mutant and sibling. (b) Injection of ddx19 mRNA rescued the morphologic defects. Compared to the control group, the experimental group rescued with ddx19 mRNA injection showed a decreased proportion of phenotypic defects ($p = 0.029$, χ^2-test). (c) The transcription level of ddx19 declined significantly in ddx19 -/- compared with its transcription in wildtype ($p = 0.007$, Student t-test). Results were preformed through three independent experiments and were normalized to β-actin, represented by mean ± SD.

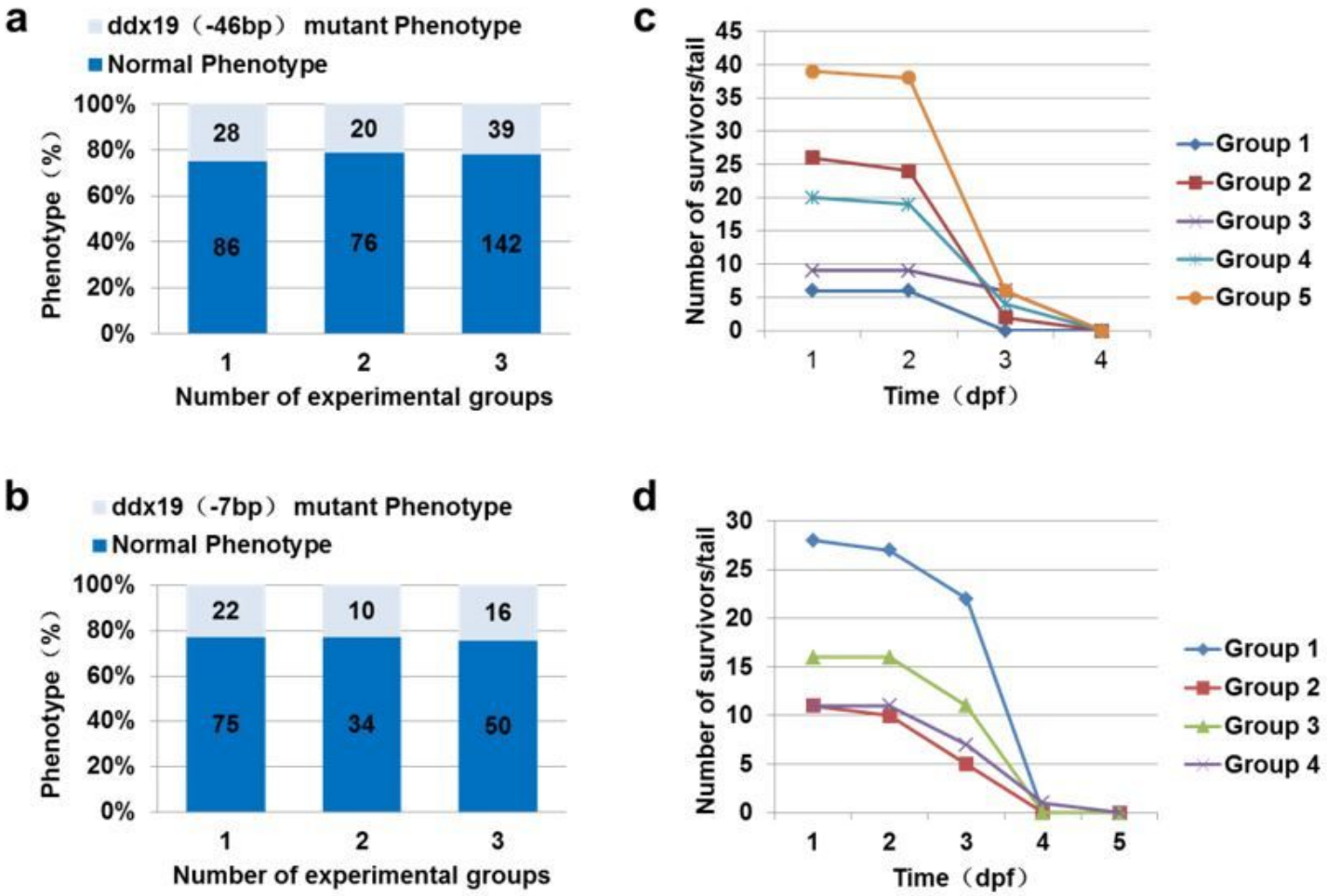

Figure 6

Phenotypes of ddx19 conformed to Mendelian's law and homozygous lethal. (a-b) Statistical results of the proportion of ddx19 -/- phenotype with 46 bp and 7 bp missing. The phenotypes consistent with Mendelian's law in the ddx19 -/- with 46 bp deletion (p = 0.970, χ2-test), and the same conclusion was reached in the ddx19 -/- with 7bp deletion (p = 0.970, χ2-test). (c) Statistical results of the viability of ddx19 -/- missing 46 bp, and the maximum survival time was up to 4dpf. (d) Statistical results of the viability of ddx19 -/- with 7 bp deletion, and the maximum survival time was no more than 5dpf

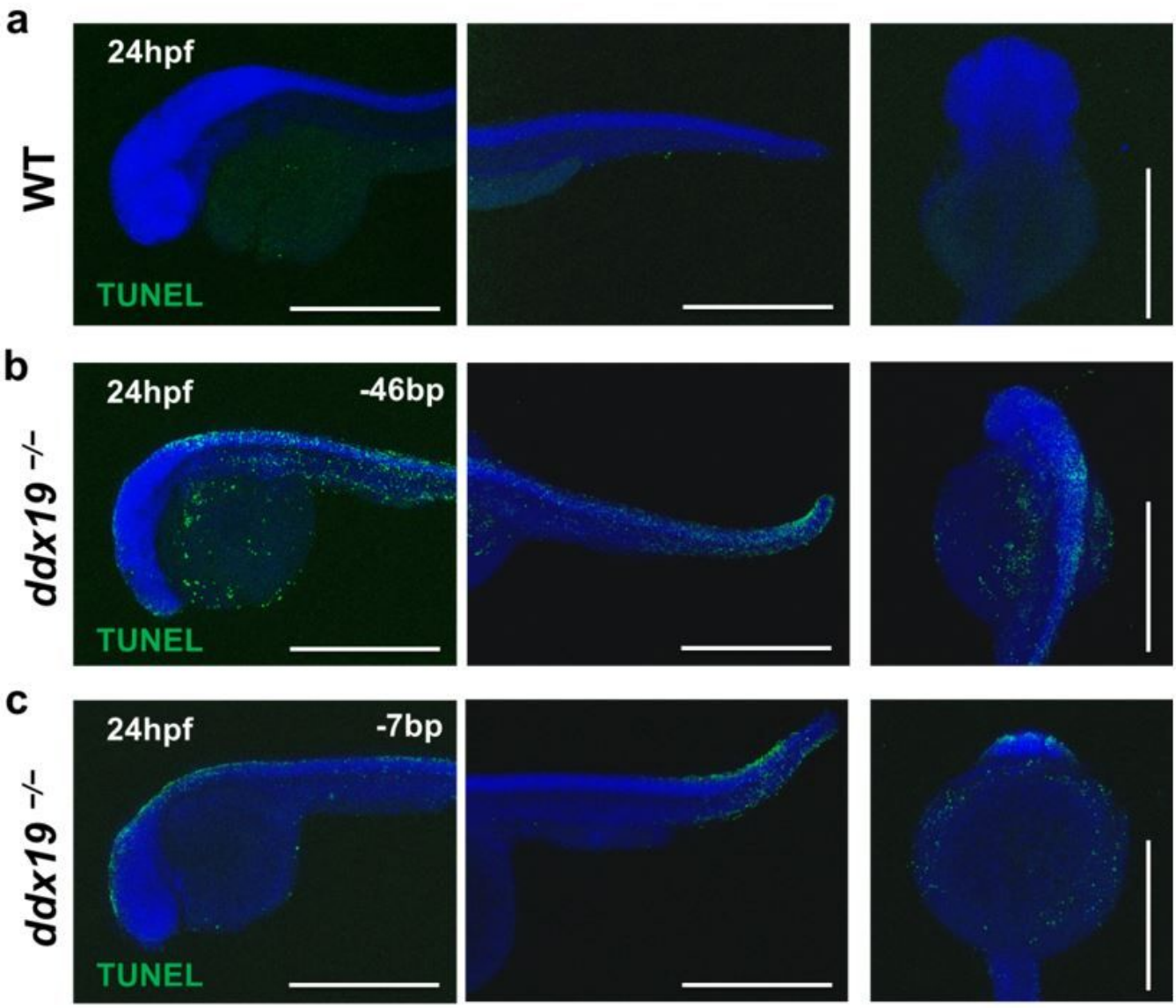

Figure 7

Two deletion types of ddx19 -/- showed widely up-regulated cell apoptosis signals. (a) Confocal imaging results of TUNEL assay in wildtype control group at 24 hpf. (b) Confocal imaging results of TUNEL assay in ddx19 -/- missing 46 bp at 24 hpf. (c) Confocal imaging results of TUNEL assay in ddx19 -/- missing 7 bp at 24 hpf. Scale bars: 500 μm.

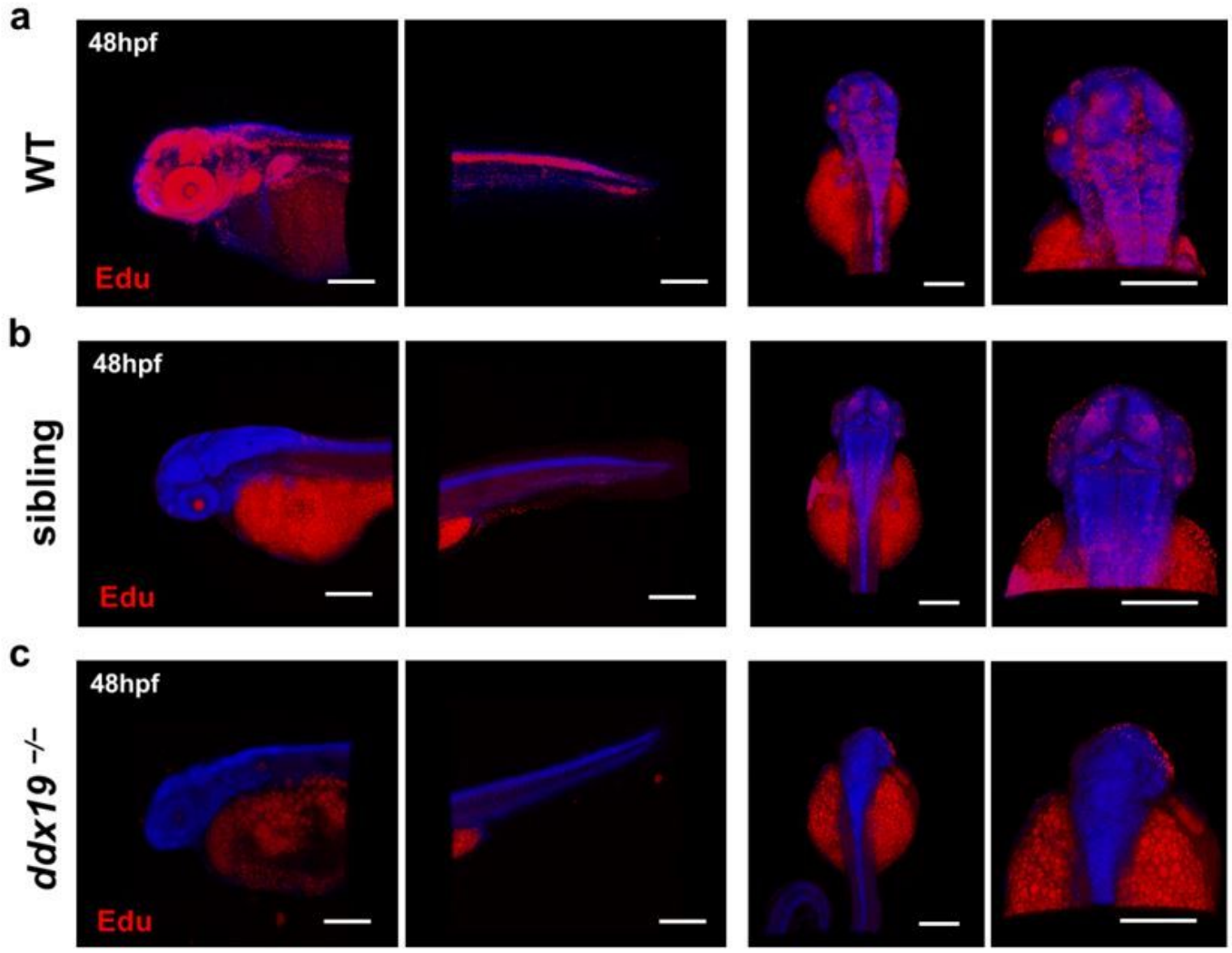

Figure 8

Cell proliferation was abnormal in ddx19 -/- at 48hpf. (a) Confocal imaging of cell proliferation in wildtype cells were detected by Edu assay. (b) Detected cell proliferation in sibling of ddx19 -/- by Edu assay. (c) Detected cell proliferation in ddx19 -/- by Edu assay. Scale bars represent 200 μm.

Supplementary Files

This is a list of supplementary files associated with this preprint. Click to download.

- Additionalfile.docx
- NC3RsARRIVEGuidelinesChecklistfillable.pdf